

# Synchronization of spatio-temporal semiconductor lasers and its application in color image encryption

S. Banerjee,<sup>1,2,\*</sup> L. Rondoni,<sup>3,†</sup> S. Mukhopadhyay,<sup>4</sup> and A. P. Misra<sup>5,6,‡</sup>

<sup>1</sup>*Dipartimento di Matematica, Politecnico di Torino,  
Corso Duca degli Abruzzi 24, 10129 Torino, Italy*

<sup>2</sup>*Micro and Nanotechnology Unit, Techfab s.r.l., Chivasso, Italy*

<sup>3</sup>*Dipartimento di Matematica and INFN, Politecnico di Torino,  
Corso Duca degli Abruzzi 24, 10129 Torino, Italy*

<sup>4</sup>*Army Institute of Management, Judge's Court Road, Alipore, Kolkata-700 027, India*

<sup>5</sup>*Department of Physics, Umeå University, SE-901 87 Umeå, Sweden.*

<sup>6</sup>*Department of Mathematics, Siksha Bhavana,  
Visva-Bharati University, Santiniketan-731 235, India*

(Received 13 October 2010; Revised 22 November 2010; Accepted 22 December 2010)

## Abstract

Optical chaos is a topic of current research characterized by high-dimensional nonlinearity which is attributed to the delay-induced dynamics, high bandwidth and easy modular implementation of optical feedback. In light of these facts, which adds enough *confusion* and *diffusion* properties for secure communications, we explore the synchronization phenomena in spatiotemporal semiconductor laser systems. The novel system is used in a two-phase colored image encryption process. The high-dimensional chaotic attractor generated by the system produces a completely randomized chaotic time series, which is ideal in the secure encoding of messages. The scheme thus illustrated is a two-phase encryption method, which provides sufficiently high confusion and diffusion properties of chaotic cryptosystem employed with unique data sets of processed chaotic sequences. In this novel method of cryptography, the chaotic phase masks are represented as images using the chaotic sequences as the elements of the image. The scheme drastically permutes the positions of the picture elements. The next additional layer of security further alters the statistical information of the original image to a great extent along the three-color planes. The intermediate results during encryption demonstrate the infeasibility for an unauthorized user to decipher the cipher image. Exhaustive statistical tests conducted validate that the scheme is robust against noise and resistant to common attacks due to the double shield of encryption and the infinite dimensionality of the relevant system of partial differential equations.

arXiv:1102.2775v1 [physics.optics] 14 Feb 2011

---

\*Electronic address: [santo.banerjee@polito.it](mailto:santo.banerjee@polito.it)

†Electronic address: [lamberto.rondoni@polito.it](mailto:lamberto.rondoni@polito.it)

‡Electronic address: [apmisra@visva-bharati.ac.in](mailto:apmisra@visva-bharati.ac.in)

## I. INTRODUCTION

The immense proliferation of internet and the advancement in telecommunication has led to vulnerability problems in securely communicating the information. Confidentiality of data and information are thus an area of concern for many researchers. An efficient and faster new breed of encryption technique operating in the physical layer of the transmission system is lately creating a lot of buzz. Quantum Cryptography and Chaos Cryptography are subtle deviations from the traditional methods of encryption techniques which are lately among the top research flurry. The first primarily focuses on quantum key distribution. The second method deals with the scrambling and transfer of encoded messages at a very high encryption data rate up to several tens of Gb/s, unlike other software based traditional schemes. This method of chaos cryptography is the outcome of the phenomenal work of chaos synchronization demonstrated by Pecora and Carroll [1]. This bifurcation from the traditional methods of encryption realized with the synchronization of two coupled chaotic trajectories opened a whole new dimension for cryptographic applications [2-7]. Its principle of operation relies primarily on the fact that the chaotic nonlinear oscillator plays the role of a broadband signal generator and the chaotic waveform can mask the information. The most distinct feature of chaotic dynamics is that they possess ergodicity [8], sensitivity to initial condition, randomness and mixing. These are the key properties which are exploited in communication theory for secure transmission of data. The experiment conducted by Cuomo and Oppenheim [9] demonstrated the feasibility of such a communication scheme suggesting that the unpredictability of chaotic oscillations of synchronized systems can be used effectively to encrypt information-bearing signals, while their deterministic nature can be used in decryption. In communication theory, a waveform which is coupled with another can be formed as a carrier over the communication channel. Here, due to chaos synchronization, the receiver end can retrieve the embedded information.

On the other hand, in order to design an efficient cryptographic system, it is imperative to select a system which is of high dimension and remains chaotic in a continuous range of the parameter space [10]. Moreover, the encryption methodology used to develop an efficient cryptic system should incorporate properties like a huge key space [11], which should be very sensitive to any kind of perturbations and immune from statistical attacks. Chaos based cryptography renders the cipher deterministically disordered having a strong dependence on even minimal variations of initial conditions and parameter values, and makes them resistant to most of the attacks.

In apropos to the above discussion, another secure method of communication can be realized at the physical layer itself by using chaotic carriers obtained from semiconductor lasers to encode an information. Reference [12] elicits that these nonlinear systems on synchronization have tremendous potential to achieve enhanced security where they play the role of emitter and receiver system when subjected to a high injection strength [13]. It is well known that, higher the complexity of the chaotic carrier the more difficult will be to decode the message without the appropriate receiver because of the high frequencies and the large number of degrees of freedom of the chaotic carrier. It is worth noting that the chaotic carriers in semiconductor diode lasers provide a broad spectrum in which the message can be hidden. With the advent of high speed telecommunications and advancements in computer processing [14] technology, the demand for faster communication is fulfilled with these laser systems which are increasingly used in major applications.

Researchers are now looking at ways to exploit lasers with chaotically fluctuating signals, to add an extra layer of privacy to messages sent over fiber-optic lines. Such optical systems will generate a chaotic carrier with considerable high dimensionality which will enhance the security level together with very high transmission rates. These higher dimensional nonlinear devices exhibit nonlinear dynamical behavior with fast irregular pulsations of the optical power, or wavelength hopping, with bandwidth ranging from a few giga-hertz to tens of giga-hertz, large correlation dimension of chaotic carriers [15,16] preventing linear filtering and frequency-domain analysis, complexity and unpredictability of the chaotic carriers, compact and integrated devices, high dimension due to the delay-induced dynamics [17] etc. In recent years, experiments were conducted with optical chaos based communication involving fiber lasers [18] and semiconductor lasers [19]. Then Argyris et al [20] in 2005 established high speed optical communication of 1Gbps over a commercial fiber-optic channel. This was a pivotal point in improved communication over other commercial and common used modes of data transmissions. The chaotic optical setup generated an optical carrier to encode and transmit a message over a communication distance of 120 km achieving a robust transmission system, immune to perturbations and channel noise. A major requisite for optical cryptography is to convert the message to be sent into an optical signal.

In order to realize secure communications using semiconductor lasers, the emitter must exhibit a chaotic regime which is subjected to chaotic oscillations by either injection from another source [21] or by reflection from an external mirror [22]. This can be achieved by when the emitter is either subjected to an optical or an electro-optical feedback. Our system is used as an optical feedback, illustrated in Fig.1, with emitter and receiver semiconductor lasers unidirectionally coupled. The setup consists of semiconductor lasers which are biased above a threshold level. These are then subjected to optical feedback using external mirrors. The receiver operates as the emitter under similar conditions in a closed loop or under CW when decoupled by open loop scheme. A piezo transducer is employed when

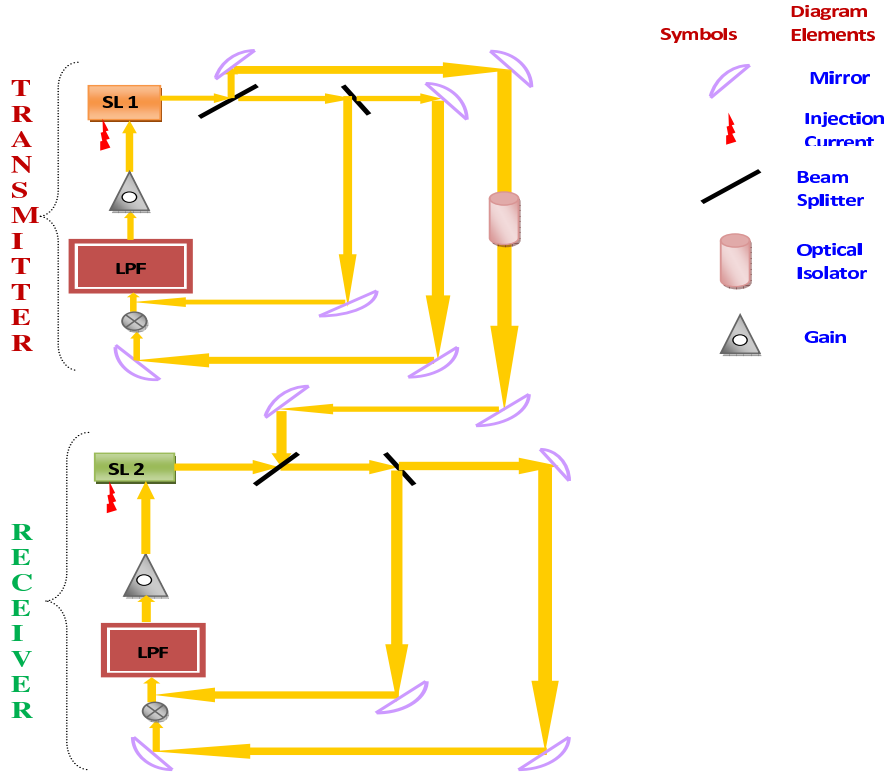


FIG. 1: (color online) Schematic diagram depicting communication scheme with two semiconductor lasers subjected to optical feedback with the emitter and receiver lasers being coupled unidirectionally.

working in a closed loop scheme, so as to match the external cavities. The optical signal thus produced is fed into a laser that passes it along the laser beam. Then chaotic synchronization occurs between the two spatially separated semiconductor lasers wherein the receiver side tunes its oscillations to that of the emitter but suppressing the hidden information. At this stage, the message is encrypted into the chaotic carrier.

Synchronization basically implies that the receiver can reproduce the exact chaotic irregular orbit of the emitter, i.e. the transmitter and the receiver both generate the same chaotic signal by reproducing the irregular time evolution of the same chaotic carrier, which traces a chaotic orbit at the emitter end. Then the chaotic carrier wave within which the message is embedded is transmitted from the emitter laser to an almost identical laser, which forms the receiver section. The output of the receiving laser is tuned to match the incoming signal from the transmitter. During decryption, the laser in the receiver section only recognizes the chaotic mask of the incoming information-bearing signal and extracts the originally transmitted message. It extracts the message by subtracting the emitter laser beam (the input), which contains the message from the identical carrier (output) generated at the receiver.

Considerable research [23-25] shows how efficient optical feedback laser systems are. In 1997, the authors [26] applied synchronization of the optical chaos from external reflection technique based on optical feedback for a robust cryptographic application by chaotic shift-keying, which is resistant to external perturbations and noise. There have been other significant successful attempts in chaos based optical communication and its application in cryptography [27-34]. However, there are other issues to be addressed regarding the reliability and efficiency of optical cryptography, concerning parameter mismatch, noise, dispersion and modulation index of chaotic carriers. Note, that the parameter mismatch has to be prevented since the correct decoding at the receiver section intrinsically depends on the tuning accuracy of the master and slave semiconductor lasers [35]. To facilitate decryption the chaotic system possesses identical parameters and operating conditions. If there is any mismatch, the devices will not be synchronized and hence will not fulfill the goal of cryptography. Moreover, the scheme has to overcome the hurdles imposed by the high-frequency together with the high dimensionality of the chaotic signal.

Another important issue is the noise produced in the lasers or in the channel communication. Such noise will hamper the accuracy of the synchronization due to which the synchronization succumbs to destabilization. Then, the dispersion factor of a chaotic laser is also an area of concern. The chaotic signal is highly sensitive to dispersion, since it has a broad line width in the order of Giga Hz in comparison to the output radiation of a solitary laser which has a line width of only few Mega-Hz. Therefore, due to the increased line width, the fiber communication links should be

shorter than the traditional ones [36] to facilitate propagation by chaotic semiconductor lasers. Lastly, the modulation index of the encryption should be small to achieve enhanced security.

In this paper, we have endeavored to use synchronized optical feedback induced chaotic dynamics for color image cryptography. The latter uses an external cavity semiconductor laser on the transmitter side and a semiconductor laser with optical injection on the receiver side. Image cryptography is achieved by forming different masks derived from preprocessed chaotic sequences arranged in the form of an image whose elements are chaotic sequences.

In the case of the two lasers, one should note that both systems are highly nonlinear and infinite dimensional in nature, even if one may only simulate a finite dimensional approximation, in a computer. The respective dynamics are also very sensitive to initial conditions, but it is possible to synchronize the two systems with a proper optical feedback mechanism. As we know, the synchronization of two continuous spatiotemporal PDE systems are quite a new subject of investigation. So, in our study, we have found interesting results which may motivate a new line of research in cryptography.

It is remarkable that, although both systems are infinite dimensional, they may easily synchronize with different initial and boundary conditions, using proper one way couplings. The experimental setup can be implemented as illustrated in the paper (Fig. 1) and the synchronization phenomenon between two lasers can then be used for practical purposes. The cryptographic scheme is just an example of the possible applications in the field of communication, which profits from the features of the system. The differences between any synchronized chaos based cryptosystem and our scheme are the following [1]:

1. The driving and the response systems are highly nonlinear and infinite dimensional in nature. Once the two systems synchronize, they remain synchronized forever. If we have synchronization at  $t = t_{max} = 5$  (dimensionless unit), they will remain the same for any  $t_i > t_{max}$ . Therefore, both the sender and receiver can start collecting data from any time after  $t_{max}$ . They can choose the data in an infinitely long time interval.
2. We have three variables in our main PDE system [Eq.(1)] viz. the forward field  $E_{+1}$ , the backward field  $E_{-1}$  and the normalized carrier density function  $N$ . The keys used to encrypt/decrypt the image file are the variables  $E_{\pm 1}, E_{\pm 2}$  and  $N_1, N_2$  respectively. The interesting thing is that the driving signal from sender to receiver constitutes a one way coupling and contains only the electric fields (eq 4) of the driving system; it does not contain any information about the carrier density. In this equation,  $N_1$  as well as  $N_2$  are not transmitted. Hence, the set of keys are

Private/ secret key for transmitter  $\rightarrow N_1$   
Private/ secret key for receiver  $\rightarrow N_2$   
Private key for both parties  $\rightarrow t_{max}$

Public key for the transmitter  $\rightarrow E_{+1}, E_{-1}$   
Public key for the receiver  $\rightarrow E_{+2}, E_{-2}$

3. Therefore, any third party attempting to hack the signal sent from the transmitter to the receiver, will only get information about the electric field  $E$  but not about the carrier density, which is used as our secret keys for encryption. They can try to reconstruct the phase space on the basis of the data obtained from the time series of the electric field  $E$ , but it is impossible to predict the nature of such a infinite dimensional PDE system.

These considerations motivated to exploit the potential of such a complex system in secure communication. The pre-requisites for any cryptographic application are met by our scheme: the system is high dimensional, guaranteeing an enormous key space, and is highly sensitive to minute perturbations, since it is spatio-temporally chaotic. This justifies consideration of our method for cryptographic applications. The system which is used to devise the algorithm for cryptographic application generates an infinite key space.

- So after synchronization, and after the time  $t_{max}$ , a state  $y_0$  is chosen, from which two sets consisting of infinitely many numbers,  $Y^1$  and  $Y^2$ , are generated.
- A key should be large enough that a brute force attack (possible against any encryption algorithm) is infeasible, i.e. would take too long to execute. According to Shannon's work on information theory, in order to achieve absolute secrecy, it is necessary for the key length to be at least as large as the message to be transmitted and

---

[1] Detailed definitions of the quantities which we briefly mention here are given in the following sections.

should be used once. This algorithm is called the One-time pad, also known as the Vignere cipher. Since longer symmetric keys require exponentially more work under brute force search, a sufficiently long symmetric key will prevent this type of attack. In our scheme, the key length is as large as the message which is transmitted [Eqs. (6),(7)]. Through the modulo operation, the length is restricted to the range  $[0, M]$  or  $[1, M+1]$ . These processed keys are of the same length as that of the message and are used exactly once and therefore this organization is theoretically unbroken [4]. So, the advantage of the Vignere cipher is reaped by our scheme. Then in order to encode an image of length  $M \times N$ , we convert the set  $Y^1$  and  $Y^2$  into a chaotic sequence  $K_1$  and  $K_2$  respectively containing the  $M \times N$  elements as that of the plain image  $P$  of dimension  $M \times N$ . Each element of the set  $K_1$  and  $K_2$  are integers in the range  $[0, M]$  or  $[1, M+1]$ . This conversion is through eq. 6 and eq 7. For example as illustrated later, with a  $512 \times 512$  sized colored image  $P$  we have restricted the key space. We obtain a set for  $P$  by transforming  $y_0$  into an array of integers in the range  $[0, 512]$  from the processing steps in Eqs. (6) and (7).

- Although, chaos is an irregular motion, it is deterministic and therefore the original image can be completely recovered if the secret keys are exactly known. But in our scheme, two of the four secret keys, the carrier density and  $t_{max}$  are not transmitted over the network and only the algorithm is assumed to be public. As a result, our scheme adheres to the Kerckhoff's principle for cryptographic algorithms.

The rest of the paper is organized as follows. In Section. II, we define a set of spatiotemporal partial differential equations (PDEs) that describes the dynamics of semiconductor lasers. The system exhibits chaos for some particular values of the parameters. In Section. III, we have implemented the synchronization phenomena in a set of coupled PDEs with linear feedback coupling. The physical significance and the results are described in detail. Section IV presents the encryption scheme based on the synchronized system of PDEs. We study the security analysis of the proposed cryptosystem with some statistical analysis in Section. V. Finally, Section. VI reports our conclusion.

## II. SPATIOTEMPORAL SEMICONDUCTOR LASERS AND THEIR CHAOTIC PROPERTIES

A spatiotemporal chaotic system is a spatially extended system that exhibits spatiotemporal chaos (STC), i.e. higher disorder in both space and time. The disorder in space can be related by rapid decay of spatial correlations whereas the temporal disorder can be measured by the positive Lyapunov exponents. Examples include the one dimensional coupled map lattices CML, which are discrete-time and discrete-space dynamical systems consisting of nonlinear maps acting on the lattice sites, coupled with each other. Because of the nonlinear dynamics of each local map and the diffusion due to the spatial coupling, a CML exhibits STC [37]. Another example of a system exhibiting spatiotemporal chaotic regime is the semiconductor laser system. The advancements in telecommunications have opened up a new arena in the study of nonlinear systems which include the high nonlinearity demonstrated by laser systems. Individual chaotic systems are often marred by the problem of rapid degradation of the chaotic dynamics in finite computing precision [38]. It is in this area that spatiotemporal systems have found an edge, for such chaotic systems have a sustained periodicity [36] with a performance superiority in cryptography [39].

Investigations with optical systems have revealed that the dynamics of laser systems with optical feedback depends on the size of the external cavity. The semiconductor lasers have been found to oscillate with several longitudinal modes simultaneously [40]. Such multimodal behavior increases the dimensionality of the rate equations and has been extensively used in applications, such as fiber couplers or compact discs. This is because semiconductor lasers have short external cavities. To realize this, one places an external reflector which feeds back a fraction of its delayed electromagnetic output into the active layer of the semiconductor laser. If the distance between the reflector and the output facet of the semiconductor laser is  $L_{ext}$ , then the round-trip time in the external cavity is  $2L_{ext}/c$ . A convenient model of this configuration should be imperatively made in the field representation, because the phase of the coherent laser radiation is strongly affected by the delayed feedback. Therefore, the system we consider takes the following form [41].

$$\begin{aligned} \pm \frac{\partial E_{\pm}}{\partial z} + \frac{\partial E_{\pm}}{\partial t} &= i \left( \frac{D_p}{L_c} \right) \frac{\partial^2 E_{\pm}}{\partial z^2} - iWL_c E_{\pm} + \kappa [(N-1) - i\alpha N] E_{\pm}, \\ \frac{\partial N}{\partial t} &= \left( \frac{D_f T}{L_c^2} \right) \frac{\partial^2 N}{\partial z^2} + \frac{\Lambda T}{N_0} - \frac{T}{\tau} N_2 - aTE_0^2 (N-1) (|E_+|^2 + |E_-|^2), \end{aligned} \quad (1)$$

where  $E_{\pm}$  are the forward (backward) electric fields normalized by the electric pump  $E_0 \sim 10^{17}$  v/m and  $N$  is the carrier density normalized by  $N_0$ . The space and the time variables are normalized respectively by  $L_0 \sim 1\mu$  m and  $T \sim 0.01$  ns. The system of Eqs. (1) describes the weakly nonlinear dynamics of slowly varying two counter

propagating longitudinally high-frequency (hf) optical fields (traveling waves) interacting with low-frequency (lf) density perturbations associated with the electron-hole (total) charge carriers in the active semiconductor lasers. In the case of a conservative system, the formation of optical envelope solitons through the nonlinear interactions of such waves is most important in the context of turbulence (in which energy is transferred to few interacting wave modes) as well as in stable optical pulse propagation. Here the amplitude of the optical wave envelope is modulated by the electrostatic small but finite amplitude electron-hole density fluctuations in which  $n_l$  represents the refractive index of the active layer,  $D_p$  the diffraction which provides higher-order dispersion. All other parameters and the corresponding numerical values for exhibiting chaos are given in Table I. Physically, since the coupling of the two laser strips, which is provided by the overlapping evanescent optical fields and by diffusion of electron-holes, can be changed by varying the inter-element distance, the dynamical behaviors of the twin-strip lasers can show a transition from order to spatiotemporal chaos of the optical field intensity [41]. Moreover, since the optical properties are strongly affected by the local optical fields and the properties of the charge carriers along the longitudinal directions, the dynamical behaviors of them are to be determined in a self-consistent manner as described above by the system of three PDEs. We numerically solve the Eqs. (1) by Runge-Kutta method with initial conditions as [42,43]

TABLE I: Laser Parameters for computations

Parameter	Value#1
L (Cavity length)	275 $\mu\text{m}$
w (Strip Width)	5 $\mu\text{m}$
d (Active layer Thickness )	0.2 $\mu\text{m}$
$R_1$ (Reflexivity of the front mirror )	0.15
$R_2$ (Reflexivity of the back mirror )	0.95
$R_3$ (Reflexivity of the external cavity)	0.95
$n_l$ (reflexive Index of the active layer )	3.5
,trim=0.0in 0in 0in -1.5in $\alpha$ (Linewidth enhancement gain)	5
a (gain coefficient)	$1.5 \times 10^{-16} \text{cm}^2$
$N_0$ (transparency concentrations)	$0.67 \times 10^{18} \text{cm}^3$
$\lambda$ (Laser wave length)	8000 nm
$\tau$ (nonradiative recombination time)	5ns
$\tau_{ext}$ (Round trip time for the external cavity)	830 ps
$L_{ext}$ (External cavity length)	12 cm
$D_f$ (diffusion coefficient)	30 $\text{cm}^2/\text{s}$
$D_p$ (Refraction Coefficient)	$10^{-5} \text{m}$
$\eta$ (Injected efficiency)	0.5
J (Injected current)	80/95/110/130 mA
$\alpha_{int}$ (Internal loss)	
s (Surface recombination velocity)	$10^6 \text{m/s}$
$\beta$ (output scaling factor)	1
$\Gamma$ (Confinement factor)	0.5
$n_c$ (refractive index of cladding)	3
$n_{eff}$ (Effective index)	3.5
$N_0$ (Career density at transparency)	$10^{24} \text{m}^{-3}$

$$E_{\pm}(z, 0) = E_{\pm 0} + \tilde{E}_{\pm 1} \cos(kz)/\beta, \quad N = -\tilde{N} \cos(kz)/\beta, \quad (2)$$

where  $k$  is the wave number of modulation,  $\beta$  is a suitable constant taken as  $1/500$  to ensure that the perturbation is sufficiently small,  $E_{\pm 0} = 2$  and  $\tilde{E}_{\pm 1}, \tilde{N}$  are constants of the order of unity. The numerical results are shown in Fig. 2 after the end of the simulation at  $t = 100$ . We increase the injected current from  $J = 80$  to  $130$  mA with external cavity length  $L_{ext} = 15$  cm and round-trip time  $\tau = 830$  ps. We choose the injection efficiency  $\eta = 0.8$  to assume that 80% of the carrier reaches the active region. From Fig. 2, we find that the forward as well as the backward fields are chaotic in nature along with the density perturbation, and we can optimize the maximum electric fields to obtain values greater than  $|E_{\pm}| = 20$  for both waves.

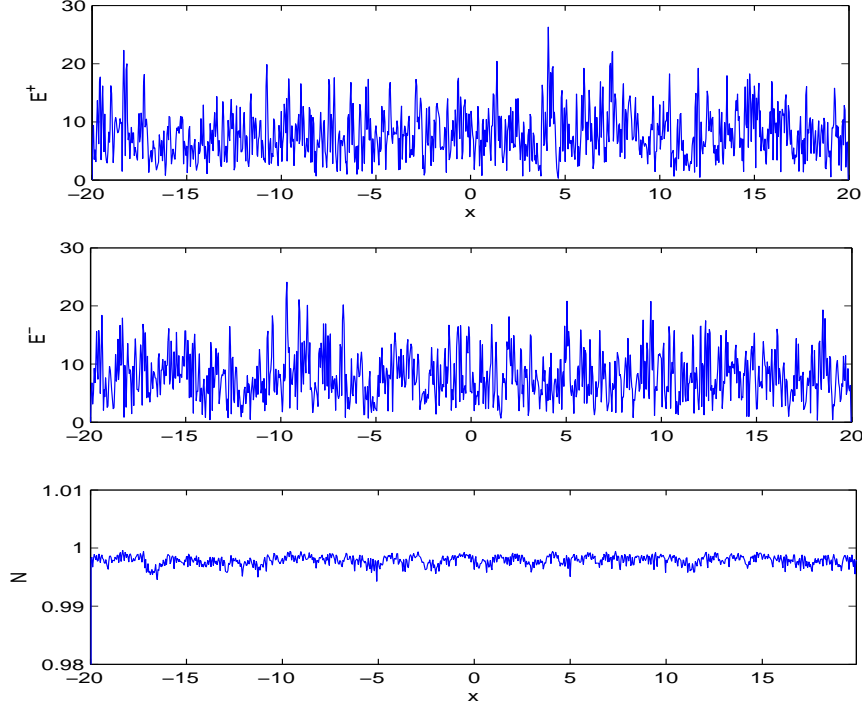


FIG. 2: (color online) Numerical solution of Eqs. (1) for forward and backward electric fields (see the upper two panels) as well as the carrier density (lower panel) exhibiting spatiotemporal chaos.

### III. SYNCHRONIZATION OF SPATIOTEMPORAL SEMICONDUCTOR LASERS

In this section we will synchronize the two nearly identical semiconductor laser systems [*c.f.* Eqs. (1)] which exhibit chaos as shown above. To this end, we use linear coupling terms with a coupling coefficient  $\epsilon$ . The former behaves like a damping rate of the optical fields in order to balance or manifest the nonlinear laser loss or gain, and can be controlled through the variation of the coupling strength  $\epsilon$ . Thus, we have the following system of equations where the suffix 1 is used to denote the driver, and 2 the response system.

$$\begin{aligned} \pm \frac{\partial E_{\pm 1}}{\partial z} + \frac{\partial E_{\pm 1}}{\partial t} &= i \left( \frac{D_p}{L_c} \right) \frac{\partial^2 E_{\pm 1}}{\partial z^2} - i W L_c E_{\pm 1} + \kappa [(N - 1) - i \alpha N] E_{\pm 1}, \\ \frac{\partial N_1}{\partial t} &= \left( \frac{D_f T}{L_c^2} \right) \frac{\partial^2 N_1}{\partial z^2} + \frac{\Lambda T}{N_0} - \frac{T}{\tau} N_1 - a T E_0^2 (N_1 - 1) (|E_{+1}|^2 + |E_{-1}|^2), \end{aligned} \quad (3)$$

and

$$\begin{aligned} \pm \frac{\partial E_{\pm 2}}{\partial z} + \frac{\partial E_{\pm 2}}{\partial t} &= i \left( \frac{D_p}{L_c} \right) \frac{\partial^2 E_{\pm 2}}{\partial z^2} - i W L_c E_{\pm 2} + \kappa [(N - 1) - i \alpha N] E_{\pm 2} + \epsilon (E_{\pm 1} - E_{\pm 2}), \\ \frac{\partial N_2}{\partial t} &= \left( \frac{D_f T}{L_c^2} \right) \frac{\partial^2 N_2}{\partial z^2} + \frac{\Lambda T}{N_0} - \frac{T}{\tau} N_2 - a T E_0^2 (N_2 - 1) (|E_{+2}|^2 + |E_{-2}|^2), \end{aligned} \quad (4)$$

where  $\kappa = \Gamma L_c N_0 a$ ,  $\epsilon = \zeta L_c$ ,  $L_c = Tc/n_l$ . Thus, the two coupled multi-mode chaotic semiconductor lasers given by Eqs. (3) and (4) describe the driver and response system respectively to demonstrate chaotic communications in high-dimensional systems through synchronization. This will enable the transmission of multiple messages through a single or multiple scalar complex field. The synchronization of the two systems (3) and (4), is achieved through the inclusion of coupling terms  $\propto \epsilon$  which, on the other way, describe non-radiative laser loss or gain by the driver or response field due to power reflectivity. It is, therefore, of importance to see whether synchronization of such high-dimensional chaotic systems is robust to noise and/ or error signals for transmitted messages. Using the similar

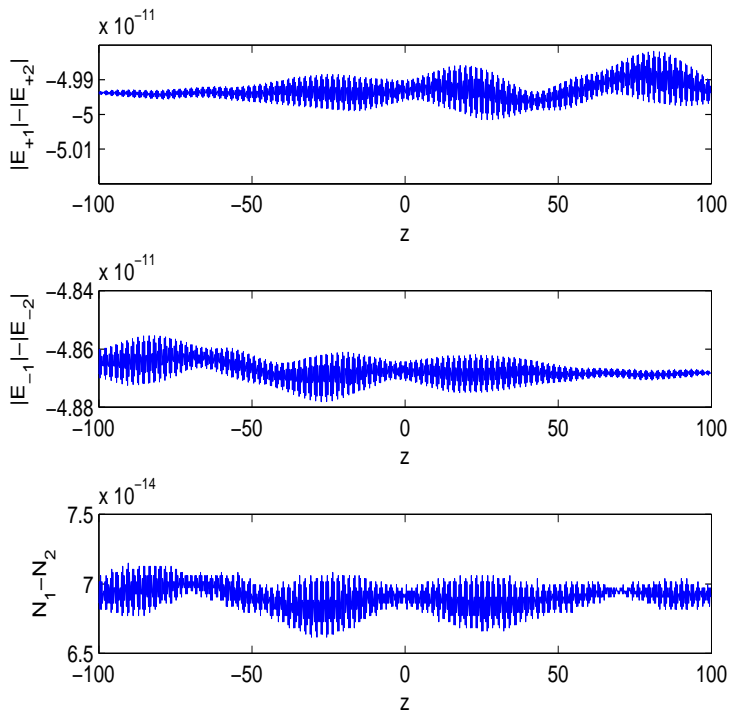


FIG. 3: (color online) Synchronization errors of coupled spatiotemporal semiconductor laser systems.

initial conditions along with  $E_{\pm}, N$  and their derivatives vanish at the boundaries, we integrate the coupled systems (3) and (4) numerically. The simulation results are displayed in Fig. 3. These basically represent the synchronization error between the driving laser (3) and the response one (4) respectively at the most chaotic state. The initial values for numerical simulation are given in Eq. (2) with  $E_{+10} = N_1 = 0.2$ ,  $E_{+11} = 1$ ,  $E_{-10} = 3$ ,  $E_{-11} = 1$ . We find that the corresponding errors for the forward and backward electric fields are of the order  $10^{-11}$  and for the carrier density the difference is of the order  $10^{-14}$ . So, at the synchronization state the system (3) can be considered as the transmitter and the system (4) as the receiver one.

#### IV. OPTICAL CHAOS AND APPLICATION TO IMAGE ENCRYPTION

This section focuses on the application of the synchronized space time laser systems to digital cryptography. Image encryption basically denotes the realignment of the pixels to different positions with a change in the statistical value of the pixels. This permutation yields a disordered version of the image which is totally incoherent. In order to realize image cryptography, it is imperative to devise a transmitter and receiver section. It is in this arena that synchronization is utilized. For cryptographic encoding, the transmitter for our scheme uses system (3) and the receiver is formed from system (4). Both of them are certain to chose values from the time series  $E_{\pm 1}$ ,  $N_1$  and  $E_{\pm 2}$ ,  $N_2$  respectively after synchronized space and time for the proposed cryptographic scheme. The proposed method is simulated in Matlab 7.0 environment.

##### A. Generation of chaos sequence

A colored digital image  $P(M, N, D)$  is basically composed of three sets of two-dimensional (2D) matrices containing integers in the range of  $0 - 255$ . Each matrix contains  $M$  number of rows and  $N$  number of columns and has three-color planes,  $D$  namely Red (R), Green (G) and Blue (B) which are concatenated along the third dimension  $D$ . Each picture element of the three-dimensional (3D) matrix in  $M \times N \times 3$  format is actually a triplet known as a *voxel*. It is analogous to its 2D monochrome image, the pixel. In this work, we would henceforth refer a picture element for a colored image as a voxel. Due to the availability of fast processing and high bandwidth technology, it is feasible to

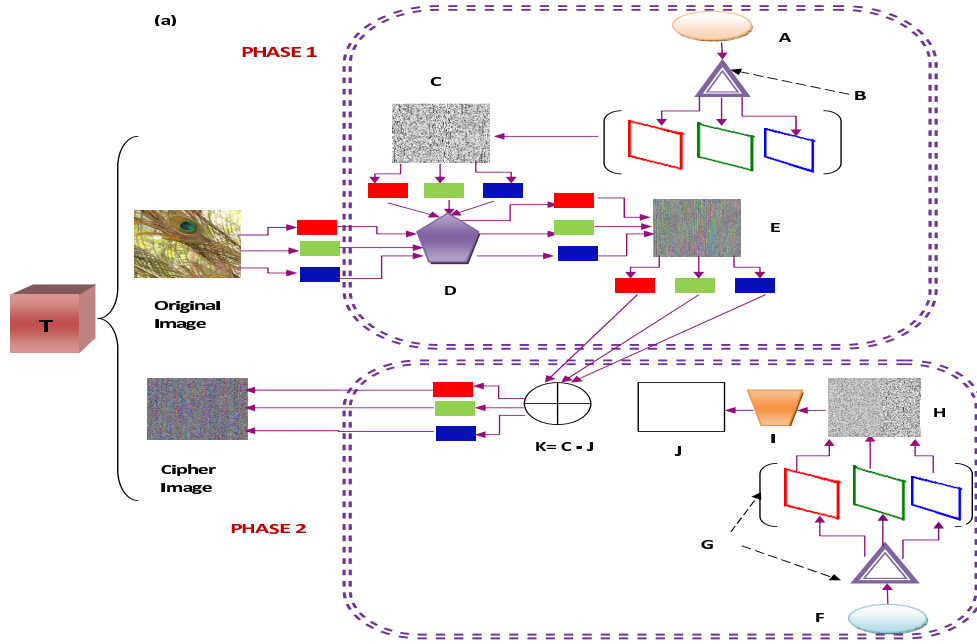


FIG. 4: (color online) Illustration of the encryption scheme: (a) Encryption by transmitter- T . Symbols :- A - Chaotic data set  $Y^1$ , B - Transformation along the color planes to form  $CSI^1$ , C - mask  $CSI^1$ , D- Shuffling operation in encryption, E - The shuffled image T, F - Chaotic data set  $Y^2$ , G - Transformation along the color planes to form  $CSI^2$ , H - the second encryption mask  $CSI^2$ , I - Transpose operation, J - The transposed mask  $CSI^{2'}$ , K - differential mask  $CSI^3$ .

employ encryption directly onto the 3D image instead of pre processing it to an indexed 2D monochrome image. This reduces considerable computational costs. Hence, the *plain image*  $P$  containing  $len = 3MN$  voxels expressed by

$$P = \{p_1 = p_1^R, p_2 = p_1^G, p_3 = p_1^B, p_4 = p_2^R, p_5 = p_2^G, p_6 = p_2^B, \dots, p_i, \dots, p_{len} = p_{MN}^B\}. \quad (5)$$

## B. The algorithm for image encryption

In digital image cryptography, Confusion and diffusion are considered as two distinct stages, both requiring image-scanning to obtain pixel/voxel values. In our method, the original message undergoes a complete randomized permutation of the positions in the diffusion phase and a drastic statistical change in the confusion phase. The proposed method eliminates the necessity of duplicated scanning thereby enhancing the encryption speed. At first, the image is partitioned into blocks of voxels. Then STC is employed to shuffle the blocks with a simultaneous change in the voxel values. Also, an efficient method for generating pseudorandom numbers from STC is suggested, which further increases the encryption speed. Theoretical analysis and computer simulations confirm that the new algorithm is highly secure and is very fast for practical image encryption.

The stream cipher mode of encryption has been implemented at the bit level with RGB image. We employ the advantages of ergodicity and sensitivity to initial conditions of synchronized chaotic system which leads to the confusion and diffusion properties required for secure cryptosystem. The entire cryptography scheme is illustrated in Figs. 4 and 5 and explained as **below**.

### Preprocessing Stages:-

1. :- The system under consideration is subjected to a maximum number of iterations  $t_{max}$ . An initial synchronized state  $y_0$  is selected to extract the chaotic sequences from variables  $E_{\pm 1}$ ,  $N_1$  at the transmitter end and  $E_{\pm 2}$ ,  $N_2$  at the receiver section. Then, the  $i$ -th chaotic data for permutation of the elements of the RGB image  $P$  of size  $3 \times M \times N$  is obtained from a synchronized data set  $Y^1 = \{y_1^1, y_2^1, \dots, y_\infty^1\}$  and  $Y^2 = \{y_1^2, y_2^2, \dots, y_\infty^2\}$  respectively from  $E_{\pm 1}$ ,  $N_1$  and are preprocessed since the elements are real numbers. The scheme employed is a duplex encryption technique. Hence, the two different data sets of keys, namely  $K^1 = \{k_1^1, k_2^1, \dots, k_\infty^1\}$

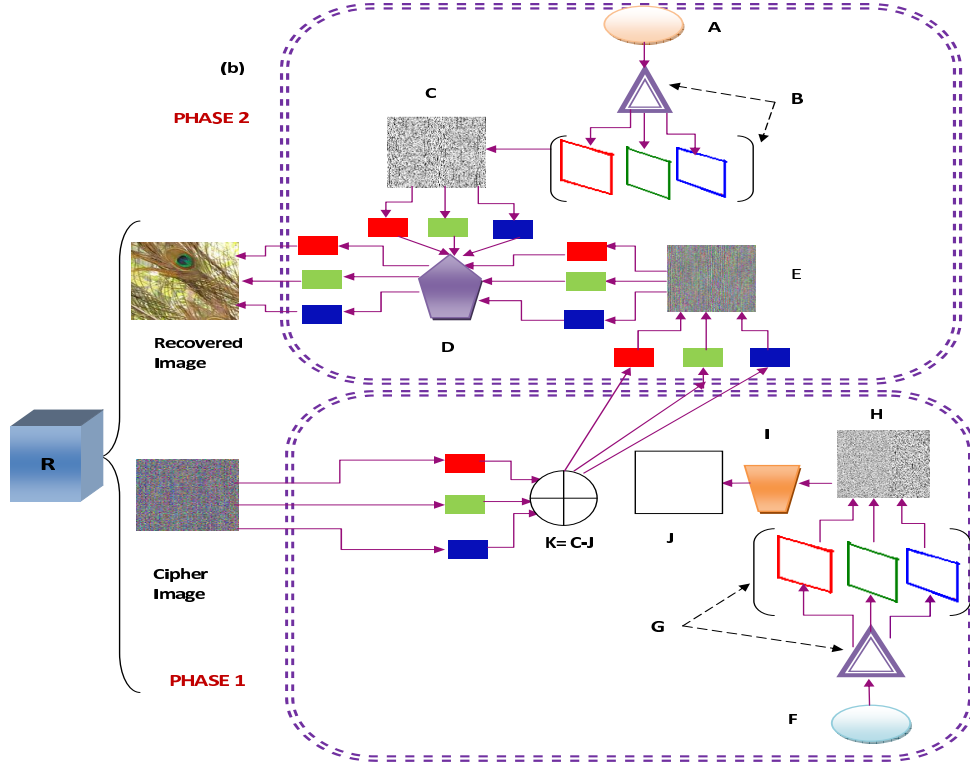


FIG. 5: (color online) Illustration of the decryption scheme: (b) Decryption in Receiver section - R. Symbols :- A - Chaotic data set  $Y^1$ , B - Transformation along the color planes to form  $CSI^1$ , C - mask  $CSI^1$ , D- Anti-shuffling in decryption, E - The shuffled image T, F - Chaotic data set  $Y_2$ , G - Transformation along the color planes to form  $CSI^2$ , H - the second encryption mask  $CSI^2$ , I - Transpose operation, J - The transposed mask  $CSI^{2'}$ , K - differential mask  $CSI^3$ .

and  $K^2 = \{k_1^2, k_2^2, \dots, k_\infty^2\}$  that are used to encrypt the image are generated through the simple algebraic relation

$$k_i^1 \leftarrow \text{integer}(\text{abs}(10^3 \times |y_i^1|)) \text{Mod}(M + 1), \quad (6)$$

and

$$k_i^2 \leftarrow \text{integer}(\text{abs}(10^5 \times |y_i^2|)) \text{Mod}(M + 1). \quad (7)$$

Hence,  $K^1$  and  $K^2 \in [0, M]$

2. :-

- Next we select a subset of integers from the processed data set  $K^1$  and  $K^2$  from Eqs. (6) and (7) into  $K^{1'}$ ,  $K^{2'}$  respectively which will now be an array of  $M \times N$  data elements with  $M$  rows and  $N$  columns and further process these through the following rules

$$K^{1'} \leftarrow \text{reshape}(K^1, M, N), \quad (8)$$

$$K^{2'} \leftarrow \text{reshape}(K^2, M, N). \quad (9)$$

where *reshape* means to change the size of  $K^1$  and  $K^2$  to  $M \times N$  array, from which the processed elements are extracted in a column wise fashion. The result of this operation will be an array containing an  $M \times N$  number of elements.

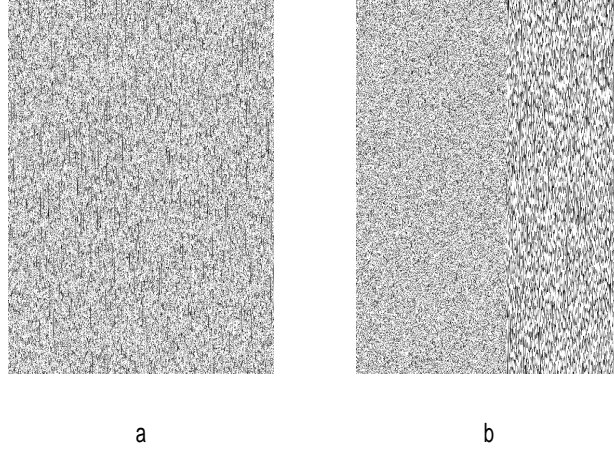


FIG. 6: (color online) The masks used in two phase cryptography: (a) Mask generated from first chaotic sequence (b) Mask generated from second chaotic sequences.

- $K^{1'}$  and  $K^{2'}$  can be represented as an image. In our scheme, we have tiled the array which have resulted from Eqs (8) and Eqs (9) along the three color planes by using the command  $repmat(X,[P Q])$  in Eqs. (10) and (11). This will produce a large array consisting of  $P \times Q$  block of array where  $X$  may be a multi dimensional array. Since, in this operation we generate an  $1 \times 3$  tilings of copies of  $K^{1'}$  and  $K^{1'}$  respectively, we denote it as equivalent to an image matrix which we label it as the Chaotic Sequence Image  $CSI_{M,N,D}^1$ ,  $CSI_{M,N,D}^2$  respectively.

$$CSI_{M,N,D}^1 \leftarrow repmat(K^{1'}, [1 \ 1 \ 3]), \quad (10)$$

$$CSI_{M,N,D}^2 \leftarrow repmat(K^{2'}, [1 \ 1 \ 3]). \quad (11)$$

Here,  $CSI^1$  will serve as the permutation mask [Fig. 6 (a)] in the diffusion stage and  $CSI^2$  [Fig. 6(b)] is used during the next phase of encryption. Each element of these phase masks are composed of chaotic sequences and therefore are completely randomized themselves.

3. :- The  $CSI^2$  is transposed into  $CSI^{2'}$  as

$$CSI_{r',c',d'}^{2'} \leftarrow CSI_{c,r,d}^2, \quad (12)$$

where by  $r' = \{1, 2, 3, \dots, N\}$ ,  $c' = \{1, 2, 3, \dots, M\}$  and  $d' = \{1, 2, 3\}$  Then the statistical difference between  $CSI^1$  and  $CSI^{2'}$  is computed as

$$CSI^3 \leftarrow \text{abs}(CSI^1 - CSI^{2'}, \text{mod}(M + 1)). \quad (13)$$

### Encryption:-

*Position Shuffling :- Diffusion phase*

Step A:-

Sort the elements of  $CSI_{r,c,d}^1$  in ascending order in accordance to their voxel values as a vector where  $r = \{1, 2, 3, \dots, M\}$ ,  $c = \{1, 2, 3, \dots, N\}$  and  $d = \{1, 2, 3\}$ . Let this be known as  $CSI_{r,c,d}^{1'}$ . Each of the elements of  $CSI^{1'}$  form the indices for position scrambling of  $P$ .

Step B:-

Shuffle all the  $M$  columns and  $N$  rows of the original image  $P(p^R, p^G, p^B)$  with  $CSI^{1'}$  into the intermediate transformation matrix  $T_{r,c,d}$  by the following simple process  
Permutation along the rows- Here we extract the pixel value of along its rows indicated by the symbol: to form the keys for row shuffling

$$k_i^1 \leftarrow CSI_{:,c,d}^{1'}$$

$$T_{r,c,d} \leftarrow P_{k_i^1, c, d}$$

Next, the columns of the intermediate resultant image is also replaced by  $CSI^{1'}$ . Permutation along the column is shown by a similar procedure where the pixel values along the column are extracted to form the keys as under

$$k_{i+1}^1 \leftarrow CSI_{r, :, d}^{1'}$$

$$T_{r,c,d} \leftarrow P_{r, k_{i+1}^1, d}$$

*Statistical Alternation:- Confusion phase*

Step C:-

In this additional phase, the matrix obtained in Eq. (13) is used to change the binary information of the image by the XOR operation represented by the symbol  $\oplus$ . Thus, the following step is executed to get the cipher image  $CI$

$$CI \leftarrow T \oplus CSI^3. \quad (14)$$

The operations discussed here occur along the three-color planes producing the final encrypted image  $CI$ . This is the cipher image which is transmitted along with the initial conditions as the secret key.

**Decryption:-**

Step D:-

The same data set  $Y^1$  and  $Y^2$  at the receiver end is preprocessed as in preprocessing steps 1 to 3. Then we perform anti-XOR and reverse permutation operation as in step A to C to recover the original image  $P$ . These procedures are lossless and reversible in nature and thus, without any overhead, we can correctly decipher the image.

## V. SECURITY ANALYSIS AND SIMULATION RESULTS

This section uses the algorithm for encrypting a  $512 \times 512$  colored image and examines its security. The bands in Fig. 7 (c) results from the abrupt changes in the diffusion process due to the inherent dynamics of the nonlinear system under consideration. It is noteworthy, that a row or a column may be permuted more than once which may be allowed since the computational cost in linear check of a duplicate value in the data set is higher than the ultimate effect of eliminating redundant position values. Figure 7(d) depicts the complete randomized orientation of the voxels making this phase totally incoherent from the original image.

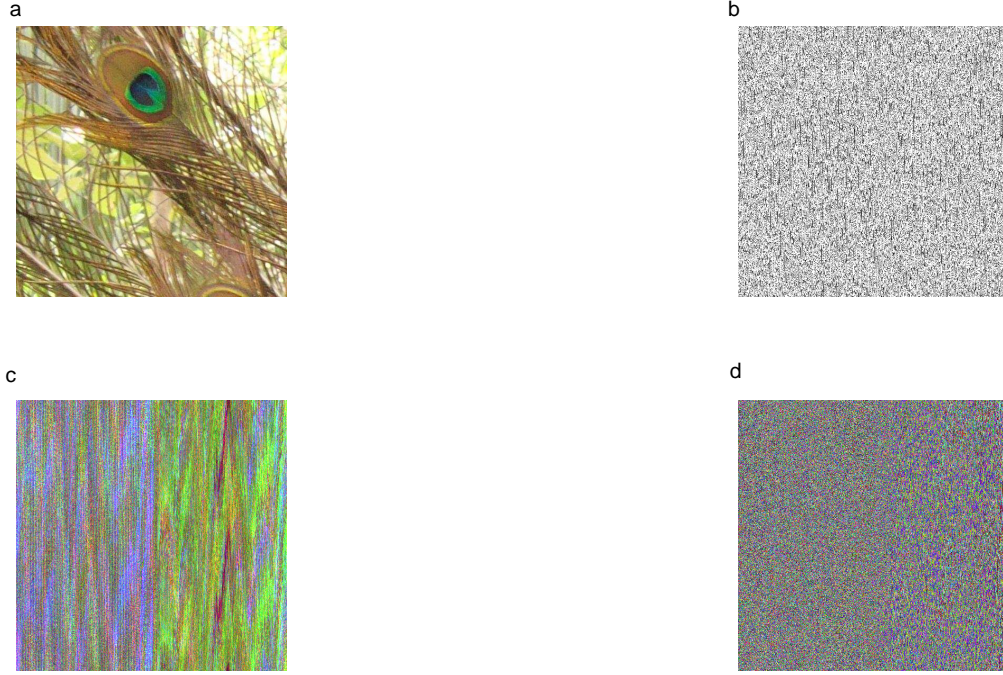


FIG. 7: (color online) The encryption process: (a) The original color image (b)The mask for permutation of original image (c) The shuffled intermediate image (d) The final cipher image.

### A. Effectiveness of the scheme

The proposed method correctly recovers the original message. This is shown by a metric known as Mean Square Error (MSE) given by

$$MSE = \frac{1}{M \times N} \sum_{r=1}^M \sum_{c=1}^N [P(r, c) - CI(r, c)]^2 \quad (15)$$

A correct recovery of the image will yield  $MSE = [MSE^R \ MSE^G \ MSE^B] = [0 \ 0 \ 0]$  for all the three-color channels separately. It is observed that the recovered image highly differs from the original with a minor change in the key set as explained subsequently.

### B. Key space attack and sensitivity analysis

For the numerical simulation of the system (3) and (4), we choose the initial conditions as

$$E_{+1}(z, 0) = E_{+10} + E_{+11} \cos(kz)/L, E_{+2}(z, 0) = E_{+20} + E_{+22} \cos(kz)/L, \quad (16)$$

$$E_{-1}(z, 0) = E_{-10} + E_{-11} \cos(kz)/L, E_{-2}(z, 0) = E_{-20} + E_{-22} \cos(kz)/L, \quad (17)$$

$$N_1 = -N_1 \cos(kz)/L, N_2 = -N_2 \cos(kz)/L. \quad (18)$$

where

$E_{+10} = N_1 = 0.2, E_{+11} = 1; E_{-10} = 0.3, E_{-11} = 1.1; E_{+20} = 0.5, E_{+22} = 1.2; E_{-20} = 0.6, E_{-22} = 1.3, N_2 = 0.5, L = 1/500, \epsilon = 2.5$  (in arbitrary units).

The total number of different keys that can be utilized in a process is termed as the key space. The 128 bit paradigm is a widely used concept in the AES cryptography scheme which is commercially used nowadays. It is a block cipher mode under the symmetric cryptography scheme. This falls under the category of traditional cryptographic technique including DES, RSA, DSA, hash functions, one time pad etc. However, our method based on a chaotic symmetric cipher stream mode of encoding the message, is an offshoot of the traditional methods of cryptography. In order to render high security, it is imperative that the key space be vast enough to make any brute force attack ineffective. Also, to ensure a large divergence of a chaotic trajectory from the initial condition, the number of iterations should be relatively large. Both these issues have been addressed. The key space with its keys are generated after a considerable number of iterations which consists of the private and the public variables viz.  $E_{\pm 1}, E_{\pm 2}$  and  $N_1, N_2$ . So, due to these keys the system has a pretty exhaustive key space which is large enough and as such makes our system resistant to brute force attacks. Each key has a value which lies within 0 – 512 for a colored image of size  $512 \times 512$ . These are used to encode the color values of the 9 bit RGB image after tiling operation along the 3 color planes according to Eqs. (8) and (9).

An encryption technique is good and efficient if the cipher image possesses sensitivity to the changes in the cipher keys, together with a combination of sufficient large key space, in order to render the system immune to major brute force attacks.

A wrong data set in any one of the stages will result an incorrect decrypted image as shown in Figs. 8 and 9. The sensitivity to keys is tested on an RGB image of size  $512 \times 512 \times 3$  through the following test cases:-

1. Test1:- Let us examine the effect of alternation of one of the secret keys at the receiver section. The original set of keys derived from variables used by the transmitter are  $E_{\pm 1}$  and  $N_1$  from Eq. (2).  $E_{\pm 1} = 0.2$  is one of the initial condition of the system which is also of the the public key. However, the initial condition values are never transmitted over the network. Now, let us assume that an attacker intercepts the communication network and self-imposes itself as the transmitter. Since, the initial conditions are never transmitted over the network, the invader attempts to make a guess about the initial conditions. In this process, let the guessed value be assumed to be  $E_{\pm 1} = 0.200001$ .

But, the key set used for decoding at the receiver section will not match with the ones used in encoding the message as the attacker has its own wrongly generated keys. So, the effect of this tampering is reflected in the incorrect recovery of the message at the receiver section in Fig. 8 (f).

2. Test2:- The keys in the permutation matrix Eq. (6) and diffusion matrix Eq. (7) are altered through the following formulae

$$k_i^1 \leftarrow \text{integer}(\text{abs}(10^6 \times |y_i^1|)) \text{Mod}(M + 1), \quad (19)$$

$$k_i^2 \leftarrow \text{integer}(\text{abs}(10^2 \times |y_i^2|)) \text{Mod}(M + 1). \quad (20)$$

The key space increases in dimension by further increasing the dimensionality during the processing stage in eq 6. In this part, we show that the keys so obtained are highly sensitive to slight change. Hence, if somehow or in a remotely possible case, another permutation matrix is generated by a third party who has gained an unauthorized access, the result will be an incorrect recovery of the message. So, the position permutation matrix is changed in Eq. (19) to display this effect of tampering without any assumption of changing or reducing the power of 10. Thus, the first key changes from 190 to 33, second key changes from 294 to 322, third from 398 to 362 and so on. The outcome is demonstrated in Fig 9 which also has high MSE values. Such high MSE values show that the image obtained by the receiver is not even close to the original and is highly uncorrelated from the original from which no visual interpretation can be deduced. Therefore, the receiver will come to know that the key set has been tampered. By Eq. (20) we have shown that the keys used in diffusion phase are equally sensitive to minute disturbances on being tampered by an attacker. So, without any specific reason for the choice of the power of 2 which is raised over 10, we have modified the key space with a reduced dimension of 10 in eq 20. The outcome is shown through the MSE values listed in Table II. Needless to say, through these exhaustive statistical tests, the sensitivity of the key sets to perturbations is validated. The effect of these are demonstrated in Fig. 9f where the decrypted image is totally incoherent from the original and there is no way to

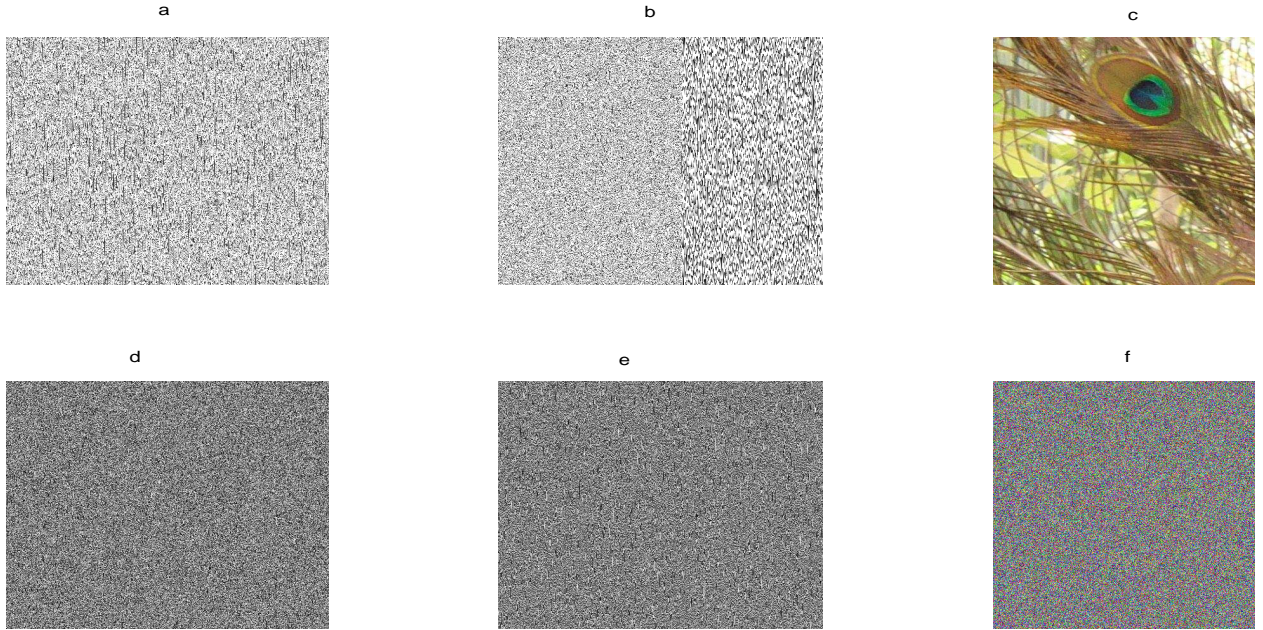


FIG. 8: (color online) Test result of statistical Test 1: (a) Chaotic phase mask  $CSI^1$  for the permutation phase with the correct keys and initial conditions (b) Second chaotic phase mask  $CSI^2$  obtained from the correct keys and initial conditions (c) Correct decrypted image (d) First chaotic phase mask for the permutation stage obtained from the incorrect keys and tampered initial conditions (e) Second chaotic phase mask obtained from the incorrect keys and tampered initial conditions (f) Incorrectly decrypted image

predict any sort of information about the original message from the incorrect recovered result. The preprocessing of the key sets along with the transpose operation of the second phase mask which is then used to form the mask image for the confusion phase adds enough stochastic properties to render the cipher image totally obscure from the original image.

TABLE II: Mean-square error for Test 1 and Test 2

MSE	R	G	B
Test1	$1.0e+003 \times 9.0296$	$1.0e+003 \times 8.6193$	$1.0e+003 \times 8.6450$
Test2	$1.0e+003 \times 9.1335$	$1.0e+003 \times 8.7111$	$1.0e+003 \times 8.5998$

The MSE value listed in Table II shows that incorrect decryption results in a very high MSE between the original and decrypted image. The values are not even closer to zero since the recovered output is remotely unrelated to the transmitted original image. Moreover, from Figs. 8 and 9 we can infer that it is almost impossible to reconstruct the original image when the secret keys and the data sets are tampered. This further reinstates that the process is immensely sensitive to small variations to the initial conditions.

### C. Differential attack resistance

A good cipher should be immune to the influence of a change in a pixel. The rate of change of the number of pixels of the cipher image  $CI$  when the plain image  $P$  is altered by just one pixel is quantified by a metric known as NPCR. It is defined by

$$NPCR = \frac{\sum_{r=1, c=1}^{M, N} D(r, c)}{M \times N} \times 100, \quad (21)$$

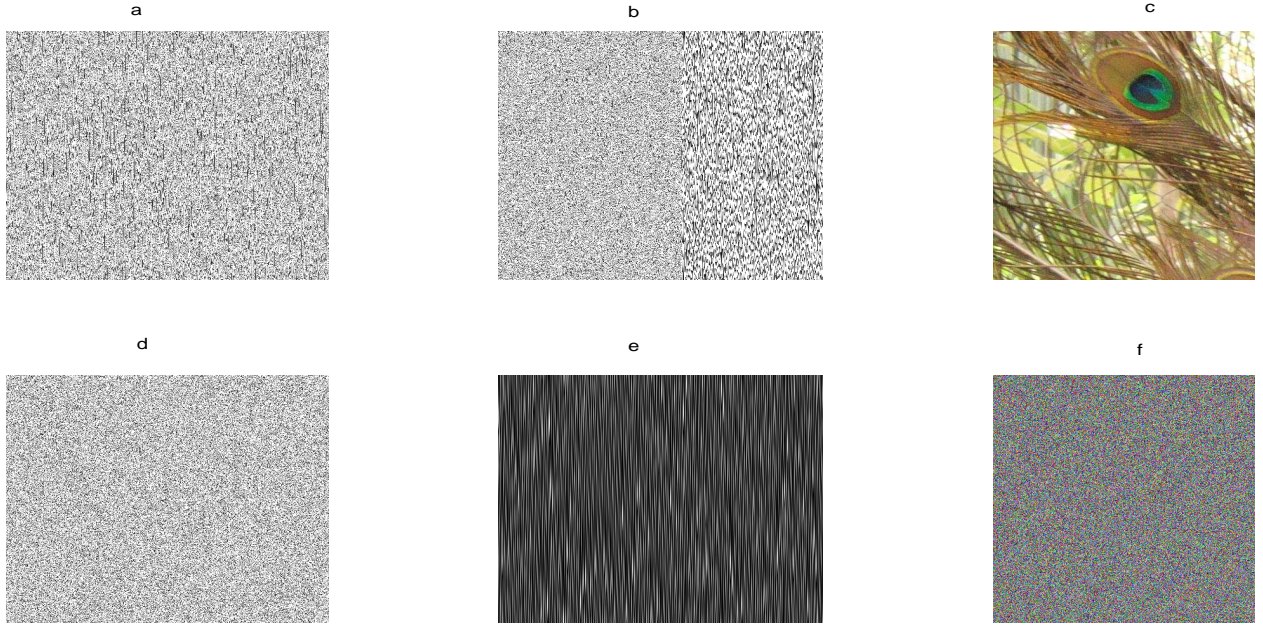


FIG. 9: (color online) Test result of statistical Test 2: (a) Chaotic phase mask  $CSI^1$  for the permutation phase with the correct keys (b) Second chaotic phase mask  $CSI^2$  obtained from the correct keys (c) Correct decrypted image (d) First chaotic phase mask for the permutation stage obtained from the incorrect keys (e) Second chaotic phase mask obtained from the incorrect keys (f) Incorrectly decrypted image.

where  $D(r, c)$  represents the change in the picture element due to encryption for a monochrome image.

$$D(r, c) = 0 \text{ when } P(r, c) = CI(r, c) \text{ else}$$

$$D(r, c) = 1 \text{ when } P(r, c) \neq C(r, c)$$

In our example, the change in a few voxel values before and after encryption are listed below to demonstrate the dispersion of voxels through the scheme

$$\begin{aligned} P(1, 1, 3) &= 153, CI(1, 1, 3) = 218, \\ P(2, 2, 3) &= 148, CI(2, 2, 3) = 74, \\ P(50, 50, 3) &= 152, CI(50, 50, 3) = 113, \\ P(100, 100, 3) &= 79, CI(100, 100, 3) = 238, \\ P(256, 256, 3) &= 42, CI(256, 256, 3) = 123. \end{aligned}$$

This shows that the resulting cipher image has its picture elements totally changed. Next quantifiable measure of diffusion properties is the Unified Average Changing Intensity (UACI) which determines the average intensity of the differences between the pixel values of the original and encrypted image. It is expressed by

$$UACI = \frac{1}{M \times N} \sum_{r=1, c=1}^{M, N} \frac{|P(r, c) - CI(r, c)|}{255} \times 100. \quad (22)$$

The results of NPCR and UACI in percentage is shown in Table III. From it we can deduce that the scheme has a high value of NPCR along with a satisfactory value of UACI. Thus, higher the value of NPCR, more is the system resistant to differential attacks. This validates the efficiency of the proposed scheme.

TABLE III: Result of differential attack: NPCR and UACI performance metric

	R	G	B
NPCR	99.61	99.62	99.60
UACI	14.47	6.97	10.35

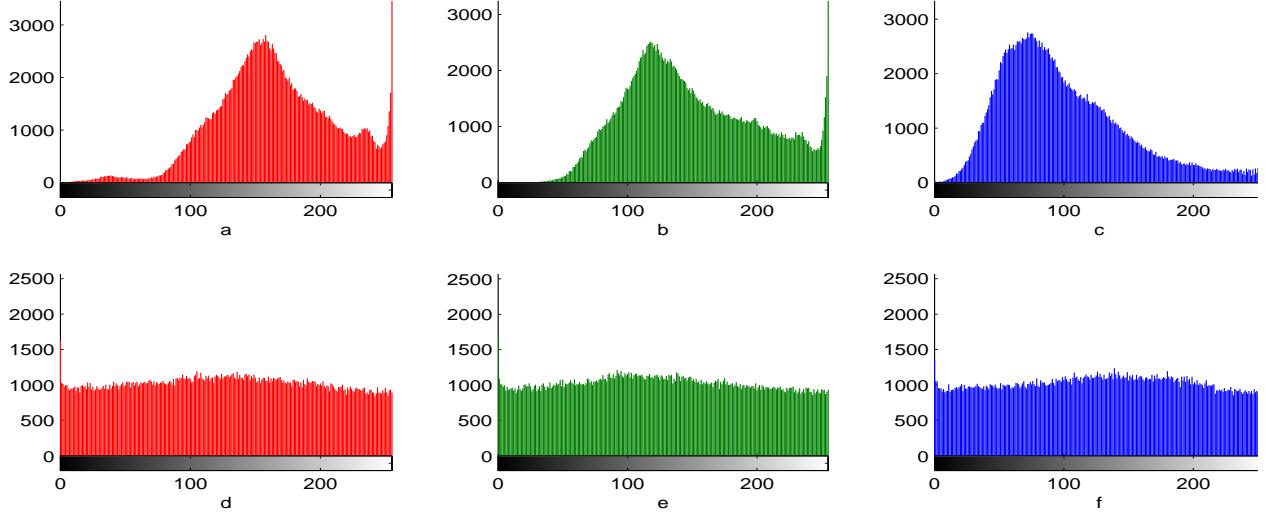


FIG. 10: (color online) Histogram: (a)-(c) original image, (d)-(e) cipher image.

#### D. Histogram analysis

The distribution of the pixels after being scrambled or manipulated can be studied with the help of a chart which represents the distribution of the pixels in the range  $0 - 255$ . For a gray image having gray level  $r_q$  it is represented by a function  $\text{hist}(l_q) = n_q$ , where  $l_q$  denotes the  $q^{\text{th}}$  gray level and  $n_q$  are the number of pixels in an image. In the diffusion phase, the positions of the image elements undergo shuffling. This does not alter the statistical information of the original image. However, the additional layer of security will disguise the desired information, as reflected in the histogram of Fig. 10. The intensity of the encrypted image greatly differs from the original image, thus an attacker will be unable to infer any statistical information required to decode from the scheme. From the result of intensity distribution, it can be ascertained that the scheme also possesses good confusion properties.

#### E. Correlation analysis of pairs of adjacent pixels

Statistical analysis of the cipher image can be performed by another excellent metric, the correlation coefficient. This shows whether there is any occurrence of an association between the guessed secret key and the observed information of the cryptosystem and forms the core information for cryptanalysis. The covariance  $\text{cov}(x, y)$  between a pair of pixel values present in the subset  $x$  and  $y$  in a gray image is defined by

$$\text{cov}(x, y) = E(x - E(x))(y - E(y)),$$

Then, the correlation coefficient  $r_{xy}$  is given by

$$r_{xy} = \frac{\text{Cov}(x, y)}{\sqrt{D(x)}\sqrt{D(y)}}. \quad (23)$$

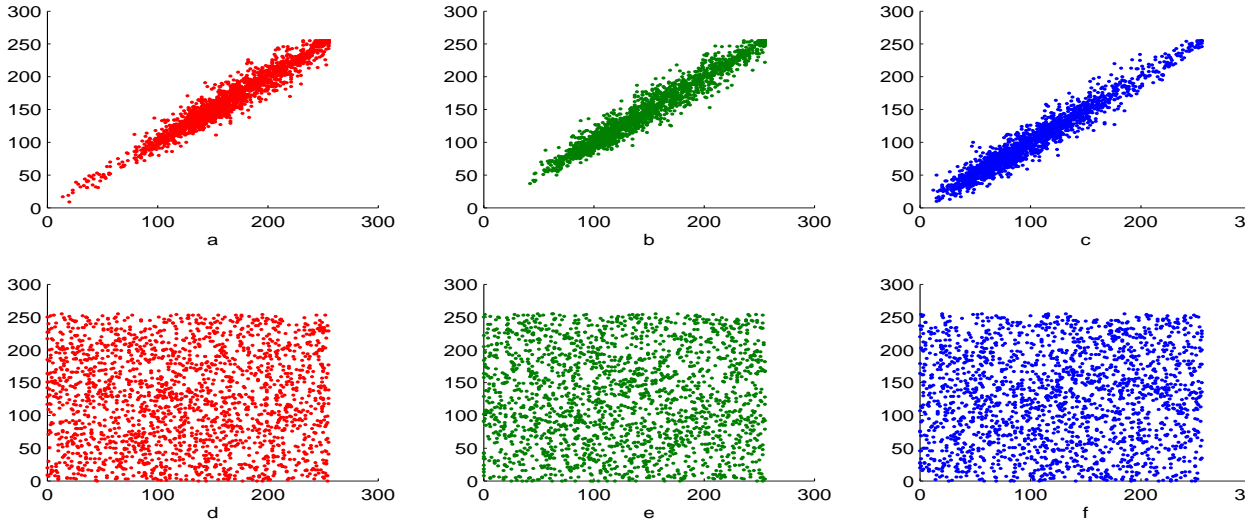


FIG. 11: (color online) Scatter plot of correlation coefficients of adjacent pairs of pixels along the horizontal direction: (a) Correlation coefficient of the original image in the Red color plane (b) Correlation coefficient of the original image in the green color plane (c) Correlation coefficient of the original image in the blue color plane.

where  $E(x), E(y)$  denotes the mean;  $D(x), D(y)$  stands for the variance between the pixels. Correlation coefficient values of a random sample of 1000 voxels, placed adjacently along the horizontal, vertical and diagonal directions, have been computed for each of the three-color channels and enumerated in Table IV. From the values, it can be observed that the correlation of cipher image is almost zero. For an efficient encryption methodology, it is imperative that the correlation values of adjacent pixels be minimal for the encoded image. Our scheme fulfills this criteria. Fig.

TABLE IV: Correlation Coefficient for each color band

	Original			Cipher		
	R	G	B	R	G	B
Horizontal	0.9714	0.9756	0.9730	-0.0002	-0.120	0.0207
Vertical	0.9592	0.9661	0.9610	0.0429	0.0539	0.0793
Diagonal	0.9621	0.9690	0.9640	0.0305	0.0270	0.0281

11 displays the spatial distribution of the randomly selected voxels from the three-color planes placed adjacently along the horizontal direction. The graphical result emphasizes that there is hardly any correlation between the original and the distorted version of the image.

## VI. CONCLUSION

The semiconductor laser represents a good amplifier configuration which exhibits stable as well as strong chaotic turbulent states. The synchronization of semiconductor lasers in their chaotic regime is still a open area of research. The corresponding system of PDEs is, infinite dimensional and continuous coupling terms necessary for the synchronization. The coupling directly injects the output power from driving system to response system. Numerical simulations show that the complete synchronization is achieved although both the systems are chaotic in nature. We have used the dynamics of the synchronized states of the system, which play the roles of the transmitter and receiver sections, in colored image cryptography. The image can be securely transmitted and recovered over the secure communication channel. The process is applied to a colored image affecting the three color planes. The key space is vast enough that attackers may very hardly guess a key. Also, the speed of encryption is notable since the

key set preprocessed before hand. The second phase of encryption with a chaotic phase mask renders the system immune to common statistical attack, even if the initial conditions are identified thereby, forming a protective shield. Furthermore, the scheme can be extended by encrypting several image maps of the chaotic data set, thereby adding several layers of security. The proposed scheme has been tested exhaustively. Statistical tests re-instate that the scheme is also sensitive to its keys and it is almost impossible to infer any information about the original image if the chaotic set is tampered with. Overall, our method is robust and found to be resistant to most of the common threats.

## Acknowledgments

LR acknowledges partial support from the European Research Council, under the European Community's Seventh Framework Programme (FP7/2007-2013) / ERC grant agreement n 202680. The EC is not liable for any use that can be made on the information contained herein. APM acknowledges support from the Kempe Foundations, Sweden.

- 
- [1] L.M.Pecora, T.L.Carroll, *Phys. Rev. Lett* **64** (1990) 821.
  - [2] L.Kocarev, G.Jakimoski, T.Stojanovski, and I.Parlitz, From chaotic maps to encryption schemes, *In Proc. IEEE Int. Symposium Circuits and Systems* **4** (1998) 514.
  - [3] L.Kocarev, Chaos-based cryptography: A brief overview *IEEE Circuits and Systems Magazine* **1** (3) (2001)6.
  - [4] S.Mukhopadhyay, M.Mitra, S.Banerjee, Chaos Synchronization with Genetic Engineering Algorithm in secure communication, In: S. Banerjee(Ed), *Chaos Synchronization and Cryptography for Secure Communications: Applications for Encryption*, IGI Global Publishers, U.S.A (2010) 476-509 ISBN-1615207376.
  - [5] G.Alvarez, G.Monotoya, F.Pastor, and M.Romera, Chaotic cryptosystems *In Proc. IEEE Int. Carnahan Conf. Security Technology*: (1999) 332-338
  - [6] L.Kocarev, Chaos-based cryptography: A brief overview, *IEEE Circuits and Systems Magazine* **1** (2001) 6.
  - [7] S.Banerjee, D.Ghosh, A.Ray and A.R. Chowdhury, *Europhysics Lett* **81** (2008) 20006.
  - [8] R.Caponetto, L.Fortuna, S.Fazzino and M.G.Xibilia, Chaotic sequences to improve the performance of evolutionary algorithms, *IEEE Transactions on Evolutionary Computation* **7** (2003) 289.
  - [9] K.M.Cuomo and A.V.Oppenheim *Phys. Rev. Lett* **71** (1993) 65.
  - [10] S.Banerjee, J.A.Yorke, C.Grebogi, Robust chaos, *Physical Review Letters* **80** (1998) 3049.
  - [11] B.Schneier, *Applied Cryptography: Protocols, Algorithm, and Source Code in C*. Wiley New York (1996).
  - [12] J.K.White and J.V.Moloney, Multichannel communication using an infinite dimensional spatiotemporal chaotic system, *Physical Review A*, **59** (1999) 2422.
  - [13] A.Murakami, Synchronization of chaos due to linear response in optically driven semiconductor lasers, *Phys. Rev. E* **65** (2002) 056617.
  - [14] K.Z.Zuo, Y.Jin, T.Xue, J.Y.Yan, Editor(s): L.I.Maoqing, ICCSE 2008, Tri-state Light Decoder of Ternary Optical Computer, *Proceedings of the Third International Conference on Computer Science & Education-Advanced Computer Technology*, New Education, (2008) 442-444.
  - [15] A.Wang, Y.Wang, and H.He, Enhancing the bandwidth of the optical chaotic signal generated by a semiconductor laser with optical feedback, *IEEE Photonics Technol. Lett* **20** (2008) 1633.
  - [16] D.M.Kane, J.P.Toomey, M.W.Lee, and K.A.Shore, Correlation dimension signature of wideband chaos synchronization of semiconductor lasers, *Opt. Lett.* **31** (2006) 20.
  - [17] K.Ikeda and K.Matsumoto, High-dimensional chaotic behavior in systems with time-delayed feedback, *Physica D* **29** (1987) 223.
  - [18] G.D.VanWiggeren, and R.Roy, Communication with chaotic lasers, *Science* **279** (1998) 1198-1200.
  - [19] S.Sivaprakasam, and K.A.Shore, Signal masking for chaotic optical communication using external-cavity diode lasers, *Opt. Lett.* **24** (1999) 1200-1202.
  - [20] A.Argyris et al., Chaos-based communications at high bit rates using commercial fibre-optic links, *Nature* **438** (7066) (2005) 343-346.
  - [21] V.Annovazzi-Lodi, S.Donati, and M.Manna, Chaos and locking in a semiconductor laser due to external injection, *IEEE J. Quantum Electron* **30** (1994) 1537-1541.
  - [22] J.Mork, B.Tromborg, and J.Mark, Chaos in semiconductor lasers with optical feedback: Theory and experiment, *IEEE J. Quantum Electron* **28** (1992) 93-107.
  - [23] M.Miinkel, F.Kaiser, O.Hess, Spatio-temporal dynamics of multi-stripe semiconductor lasers with delayed optical feedback, *Physics Letters A* **222** (1996) 67-75.
  - [24] G.Huyet, J.K. White, A.J. Kent, S.P. Hegarty, J.V. Moloney, and J. G. McInerney, Dynamics of a semiconductor laser with optical feedback, *Physical Review A* **60**( 2) (1999) 1534-1537.
  - [25] C.Serrat, S.Prins, and R.Vilaseca, Dynamics and coherence of a multimode semiconductor laser with optical feedback in an intermediate-length external-cavity regime, *Physical Review A* **68** 053804 (2003) 1-7.
  - [26] V.Annovazzi-Lodi, S.Donati, & A. Scire, Synchronization of chaotic lasers by optical feedback for cryptographic appli-

- cations, *IEEE Journal of Quantum Electronics* **33(9)** (1997) 1449-1454.
- [27] Y.Liu, H.F.Chen, J.M.Liu, P.Davis, and T.Aida, Communication Using Synchronization of Optical-Feedback-Induced Chaos in Semiconductor Lasers, *IEEE Transactions on Circuits and Systems I: Fundamental Theory and Applications* **48(12)** (2001).
- [28] C.R.Mirasso, & J.Mulet, C.Masoller, Chaos Shift-Keying Encryption in Chaotic External-Cavity Semiconductor Lasers Using a Single-Receiver Scheme, *IEEE Photonics Technology Letters* **14(4)** (2002).
- [29] V.Bindu and V.M.Nandakumaran, Chaotic encryption using long-wavelength directly modulated semiconductor lasers, *Journal of Optics A: Pure and Applied Optics* **4(2)** (2002) 115.
- [30] E.Klein, N.Gross, E.Kopelowitz, M. Rosenbluh, L.Khaykovich, W. Kinzel, and I.Kanter, Public-channel cryptography based on mutual chaos pass filters, *Physical Review E* **74** 046201 (2006).
- [31] O.A.Rossoa, R.Vicentec, and C.R.Mirasso, Encryption test of pseudo-aleatory messages embedded on chaotic laser signals: An information theory approach, *Physics Letters A* **372(7)** (2008) 1018-1023.
- [32] A.Guerreiro, Cryptographic key distribution in optical systems: quantum vs. chaos, *Transparent Optical Networks IC-TON '09. 11th International Conference on, Azores* (2009).
- [33] N.Jiang, W.Pan, L.Yan, B. Luo, L.Yang, S.Xiang, D.Zheng, Two chaos synchronization schemes and public-channel message transmission in a mutually coupled semiconductor lasers system *Optics Communications* **282(11)** (2009) 2217-2222.
- [34] A.Tomita, K.Yoshino, Y.Nambu, A.Tajima, A.Tanaka, S.Takahashi, W.Maeda, S.Miki, Z.Wang, M.Fujiwara, M.Sasaki, High speed quantum key distribution system, *Optical Fiber Technology* **16(1)** (2010) 55-62.
- [35] J.Revuelta, C.R.Mirasso, P.Colet and L.Pesquera, *IEEE Photon. Tech. Lett.* **14** (2002) 140.
- [36] S.Wang, W.Liu, H.Lu, J.Kuang, and G.Hu, *Int. J. Mod. Phys. B* **18** (2004) 2617.
- [37] P.Li, Z.Li, W.A.Halang, and G.Chen, *Chaos, Solitons Fractals* **32** (2007) 1867.
- [38] S.Li, G.Chen, and X.Mou, *Int. J. Bifurcation Chaos Appl. Sci. Eng* **15** (2005) 3119.
- [39] X.Wang, M.Zhan, C.-H.Lai, and H.Gang, *Chaos* **14** (2004) 128.
- [40] C.Serrat, S.Prins, and R.Vilaseca, Dynamics and coherence of a multimode semiconductor laser with optical feedback in an intermediate-length external-cavity regime, *Physical Review A* **68** (2003) 053804.
- [41] O. Hees and E. Scholl, *Physica D* **70** (1994) 177
- [42] S.Banerjee, A.P.Misra, P.K.Shukla, and L.Rondoni, *Phys. Rev. E* **81** (2010) 046405.
- [43] A.P.Misra and P.K.Shukla, *Phys. Rev. E* **79** (2009) 046405.